American College of Neuropsychopharmacology

ARTICLE

Check for updates

Structure-activity relationships for 5F-MDMB-PICA and its 5F-pentylindole analogs to induce cannabinoid-like effects in mice

Grant C. Glatfelter[1], John S. Partilla[1] and Michael H. Baumann[1]✉

Synthetic cannabinoid receptor agonists (SCRAs) are an evolving class of new psychoactive substances found on recreational drug markets worldwide. The indole-containing compound, 5F-MDMB-PICA, is a popular SCRA associated with serious medical consequences, including overdose and hospitalizations. In vitro studies reveal that 5F-MDMB-PICA is a potent agonist at cannabinoid type 1 receptors (CB_1), but little information exists regarding in vivo pharmacology of the drug. To this end, we examined the in vitro and in vivo cannabinoid-like effects produced by 5F-MDMB-PICA and related 5F-pentylindole analogs with differing composition of the head group moiety (i.e., 5F-NNEI, 5F-SDB-006, 5F-CUMYL-PICA, 5F-MMB-PICA). In mouse brain membranes, 5F-MDMB-PICA and its analogs inhibited binding to [^{3}H]rimonabant-labeled CB_1 and displayed agonist actions in [^{35}S]GTPγS functional assays. 5F-MDMB-PICA exhibited the highest CB_1 affinity ($K_i = 1.24$ nM) and functional potency ($EC_{50} = 1.46$ nM), but head group composition markedly influenced activity in both assays. For example, the 3,3-dimethylbutanoate (5F-MDMB-PICA) and cumyl (5F-CUMYL-PICA) head groups engendered high CB_1 affinity and potency, whereas a benzyl (5F-SDB-006) head group did not. In C57BL/6J mice, all 5F-pentylindole SCRAs produced dose- and time-dependent hypothermia, catalepsy, and analgesia that were reversed by rimonabant, indicating CB_1 involvement. In vitro K_i and EC_{50} values were positively correlated with in vivo ED_{50} potency estimates. Our findings demonstrate that 5F-MDMB-PICA is a potent SCRA, and subtle alterations to head group composition can have profound influence on pharmacological effects at CB_1. Importantly, measures of CB_1 binding and efficacy in mouse brain tissue seem to accurately predict in vivo drug potency in this species.

Neuropsychopharmacology (2022) 47:924–932; https://doi.org/10.1038/s41386-021-01227-8

INTRODUCTION

New psychoactive substances (NPS) are synthetic compounds specifically engineered to reproduce the pharmacological effects of traditional drugs of abuse while bypassing current drug control laws [1, 2]. NPS represent a diverse collection of compounds encompassing various drug classes, the total number of which has been steadily increasing over the last 10 years [3]. Synthetic cannabinoid receptor agonists (SCRAs) are a class of NPS designed to mimic the effects of 6,6,9-trimethyl-3-pentyl-6a,7,8,10a-tetrahydrobenzo[c]chromen-1-ol (THC), the main psychoactive compound in cannabis. It is well established that THC produces its psychoactive effects via low efficacy agonist actions at cannabinoid-1 receptors (CB_1) in the central nervous system [4–6]. SCRAs are one of the fastest growing classes of NPS and display substantial chemical diversity [5, 7, 8]. In contrast to cannabis use, SCRA use is associated with hospitalizations, overdose, and sometimes death [9]. The enhanced risks posed by use of SCRAs could be due to their greater potency and efficacy at CB_1, non-cannabinoid (i.e., off-target) effects, biased signaling at CB_1, or unique metabolism [4, 7, 8, 10–14]. Because SCRAs are associated with serious public health risks, and the diversity of substances is constantly evolving, there is a need for rapid examination of SCRA pharmacology as new substances appear on recreational drug markets.

Over the past few years, methyl (2 S)-2-[[1-(5-fluoropentyl)indole-3-carbonyl]amino]-3,3-dimethylbutanoate (5F-MDMB-PICA) has emerged as one of the most popular SCRAs worldwide [15–21]. 5F-MDMB-PICA is a 5F-pentylindole SCRA and close structural analog of the first generation cannabinoid compound, [1-(5-fluoropentyl)indol-3-yl]-naphthalen-1-ylmethanone (AM-2201), with modification to the linker and head group moieties (see Fig. 1) [7]. The in vitro pharmacology of 5F-MDMB-PICA was first reported in 2016 [22], it was subsequently confiscated in Europe during 2017 [23], and from 2018 – 2020 it was the most commonly detected SCRA in law enforcement drug seizures and human forensic casework in the United States of America (USA) [17–21, 24]. 5F-MDMB-PICA is commonly found in 'legal high' products such as herbal smoking mixtures [15, 23], vape liquids, or infused paper products for smuggling into prisons [25, 26], and has been associated with serious intoxications, overdose, and even death in some cases [27, 28]. Due to its propensity for adverse effects, 5F-MDMB-PICA was placed into emergency Schedule I control by the USA Drug Enforcement Administration in 2019 [29]. Despite the popularity of 5F-MDMB-PICA, only limited information is available about its pharmacology and toxicology, especially in vivo. Krotulski et al. recently demonstrated that 5F-MDMB-PICA displays low nM affinity for CB_1 in rat brain membranes [30], but scant information is available regarding efficacy of the compound in native tissue

[1]Designer Drug Research Unit (DDRU), National Institute on Drug Abuse (NIDA), Intramural Research Program (IRP), Baltimore, MD, USA. ✉email: mbaumann@mail.nih.gov

Received: 15 June 2021 Revised: 21 October 2021 Accepted: 26 October 2021
Published online: 20 November 2021

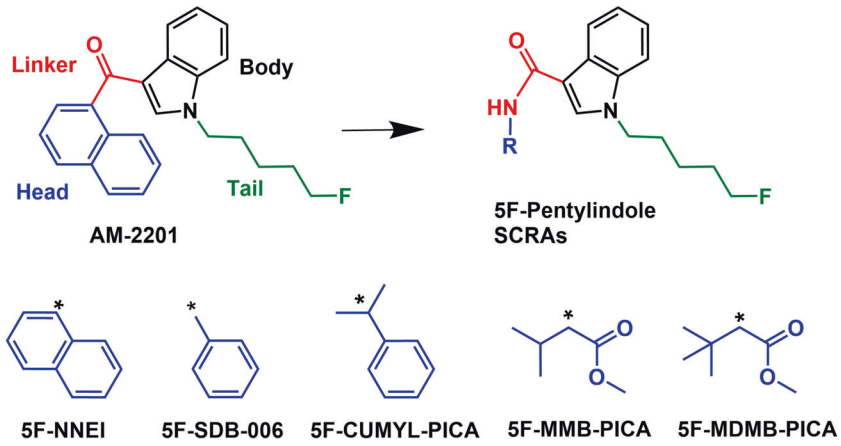

Fig. 1 Chemical structures of 5F-pentylindole synthetic cannabinoids showing linker and head group variations, as compared to the parent compound AM-2201.

preparations. Several published studies demonstrate that 5F-MDMB-PICA is a potent agonist in cells transfected with CB_1, but reported potency values vary [22, 31–33]. For example, in four different in vitro systems, 5F-MDMB-PICA displayed EC_{50} values of 0.45 [22], 0.70 [32], 3.26 [31], and 27.60 [33] nM at CB_1 receptors. The differences in drug potency across studies are likely related to the different cell-based assay platforms and specific reference ligands (e.g., CP-55,940 versus JWH-018) employed. In the case of 5F-MDMB-PICA, it is not known whether data from transfected cells reflect in vivo potency in humans or animal models, as is the case for other cannabinoids [34–37].

The present experiments were designed to examine the in vitro and in vivo cannabinoid-like effects produced by 5F-MDMB-PICA in mice. In addition, we wished to compare the effects of 5F-MDMB-PICA to a series of structurally related 5F-pentylindoles which differed only in their "head group" composition (see Fig. 1 for chemical structures). Specifically, we investigated the cannabinoid-like effects produced by 5F-MDMB-PICA, methyl (2 S)-2-[[1-(5-fluoropentyl)indole-3-carbonyl] amino]-3-methylbutanoate (5F-MMB-PICA), 1-(5-fluoropentyl)-N-(2-phenylpropan-2-yl)indole-3-carboxamide (5F-CUMYL-PICA), N-benzyl-1-(5-fluoropentyl)indole-3-carboxamide (5F-SDB-006), 1-(5-fluoropentyl)-N-naphthalen-1-ylindole-3-carboxamide (5F-NNEI), and AM-2201. First, 5F-MDMB-PICA and its analogs were tested for their ability to inhibit binding to CB_1 labeled with [^{3}H]SR141716A ([^{3}H]rimonabant) and to induce agonist actions in [^{35}S]GTPγS functional assays in mouse brain membranes. Next, the 5F-pentyindole SCRAs were tested in vivo for their ability to induce hypothermia, catalepsy, and analgesia (i.e., triad test procedure) after subcutaneous (s.c.) administration in mice. Subsequent experiments were conducted to verify the role of CB_1 in mediating in vivo cannabinoid-like effects in mice pretreated with the CB_1 antagonist, rimonabant [38, 39], prior to administration of 5F-pentylindole SCRAs. Lastly, we determined correlative relationships among K_i affinity values, EC_{50} potency values, and ED_{50} potencies from triad test procedures in mice, to assess the utility of in vitro data in predicting in vivo effects for this series of SCRAs. Our findings demonstrate that 5F-MDMB-PICA is a potent SCRA, and head group composition of 5F-pentylindole analogs can markedly affect pharmacological effects.

MATERIALS AND METHODS

Drugs & reagents

[^{3}H]Rimonabant (42 Ci/mmole) and [^{35}S]GTPγS (1250 Ci/mmol) were purchased from PerkinElmer (Waltham, MA, USA). Rimonabant, AM-2201, 5F-MDMB-PICA (also known as 5F-MDMB-2201), 5F-MMB-PICA (also known as 5F-AMB-PICA), 5F-CUMYL-PICA (also known as SGT-67), 5F-SDB-006, 5F-NNEI (also known as 5F-MN-24), and CP-55,940 were purchased from Cayman Chemical Company (Ann Arbor, MI, USA). THC was provided by the pharmacy at the Intramural Research Program (IRP) of the National Institute on Drug Abuse (NIDA) (Baltimore, MD, USA). Other chemicals and reagents were obtained from MilliporeSigma (St. Louis, MO, USA).

Animals & housing

C57BL/6J male mice (20–30 g) were purchased from The Jackson Laboratory (Bar Harbor, ME, USA) at 7–8 weeks of age. Mice were group-housed prior to experiments in a standard 12-h light-dark cycle (lights on at 0700 h and lights off at 1900 h) with *ad libitum* access to water and food. The vivarium facilities at the NIDA IRP in Baltimore, MD, USA, are fully accredited by the Association for the Assessment and Accreditation of Laboratory Animal Care. All procedures were approved by the Animal Care and Use Committee of the NIDA IRP.

[^{3}H]Rimonabant binding assay in mouse brain

Binding of [^{3}H]rimonabant to mouse brain membranes was performed as previously described with minor modifications [40]. The [^{3}H]rimonabant binding assays used a pooled membrane preparation from fourteen mouse brains. To create the membrane pool, each mouse brain (C57BL/6J strain, BIOIVT, Hicksville, NY, USA) was homogenized by 6 strokes of a motor-driven Teflon/glass homogenizer (Caframo type RZR1, Wiarton, Ontario, Canada) on setting 7, in 10 mL 100 mM Tris buffer (pH 9), containing 1 mM EDTA at 4 °C. The homogenates were centrifuged at 900 × *g* for 10 min at 4 °C, and the pellets were discarded. Supernatants were combined and aliquoted into fresh centrifuge tubes so that each tube contained the equivalent volume of material from two mouse brains. The aliquots were centrifuged at 11,500 × *g* for 25 min at 4 °C, the supernatants were discarded by aspiration, and the pellets were stored at −80 °C.

[^{3}H]Rimonabant binding assays were performed in 12 × 75 mm glass test tubes using 50 mM Tris buffer (pH 7.4 at 30 °C), containing 1 mM EDTA and 3 mM $MgCl_2$. One pellet was thawed, suspended uniformly in 1 mL buffer by repeated pipetting, and diluted to 20 mL with buffer. This preparation provided sufficient material for triplicate inhibition curves for each of the test compounds. Binding assays were initiated by the addition of 100 µL of tissue suspension (40 µg membrane protein) to each test tube that contained 400 µL of buffer with 1 mg/mL fatty acid free bovine serum albumin, test drug dissolved in DMSO (5 µL), and [^{3}H]rimonabant in DMSO (10 µL) at a final concentration of 0.25 nM. After 30 min at 30 °C, radiolabeled membranes were retained on GF/B glass fiber filters (Brandel, Gaithersburg, MD, USA) by rapid vacuum filtration using a cell harvester (Brandel). Filters were rinsed with 6 mL ice cold wash solution (0.9% NaCl containing 2 mg/mL fatty acid free bovine serum albumin), and retained radioactivity was quantitated using a MicroBeta2 liquid scintillation counter (PerkinElmer) at 40% efficiency. Binding of [^{3}H]rimonabant was proportional to the amount of membrane protein and was saturable with respect to time (5 min) and the amount of [^{3}H]rimonabant added (K_d= 0.28 ± 0.01 nM, B_{max} = 1.9 ± 0.3 pmol/mg protein).

[^{35}S]GTPγS functional assay in mouse brain

The binding of [^{35}S]GTPγS to mouse brain membranes was performed as described by De Luca, et al. [41] with minor modifications. Fresh whole

mouse brains (C57BL/6J strain, BIOIVT) were homogenized by 6 strokes of a motor-driven Teflon/glass homogenizer (Caframo type RZR1, Wiarton, Ontario, Canada) on setting 7, in 20 volumes of ice cold 50 mM Tris buffer (pH 7.0), containing 3 mM $MgCl_2$ and 1 mM EDTA. Homogenates were centrifuged at 45,000 × *g* for 10 min at 4 °C, the supernatants were discarded, and pellets were resuspended by vortexing in 2 mL of the Tris/$MgCl_2$/EDTA buffer. Membrane suspensions were centrifuged as previously described, the supernatants were discarded, and pellets were resuspended by vortexing in ice cold 50 mM Tris (pH 7.4) containing 3 mM $MgCl_2$, 0.2 mM EGTA, and 100 mM NaCl (assay buffer). Aliquots from this suspension were stored at −80 °C until the day of use. Each mouse brain provided membranes sufficient for 400 determinations.

[^{35}S]GTPγS binding assays were performed in 12 × 75 mm polystyrene test tubes. Each tube contained 1 mL assay buffer with adenosine deaminase (20 mU), fatty acid-free bovine serum albumin (1 mg/mL), GDP (30 μM), 0.05 nM [^{35}S]GTPγS, test drugs, and mouse brain membranes. Assays were initiated by the addition of [^{35}S]GTPγS and were terminated after 60 min at 30 °C by rapid vacuum filtration using a Brandel tissue harvester (Brandel) loaded with GF/B filters (Brandel) that had been pre-soaked in wash buffer (ice cold 50 mM Tris pH 7.0) for 20 min. Filters were rinsed twice with 1 mL cold wash buffer, immediately placed in 24-well plates (Perkin Elmer), and soaked overnight in 450 μL Cytoscint (MP Biomedicals, Santa Ana, USA). Radioactivity was quantitated at 95% efficiency by a Microbeta2 liquid scintillation counter (Perkin Elmer). Non-specific activity was determined in the presence of 10 μM GTPγS. Effects of test drugs on [^{35}S]GTPγS binding were expressed as % of binding in the absence of any added drug.

Transponder implants & triad test in mice

One week prior to the start of behavioral testing, s.c. temperature transponders (14 × 2 mm, model IPTT-300, Bio Medic Data Systems, Inc. Seaford, Delaware, USA) were surgically implanted into male mice under brief isoflurane anesthesia. Mice were single-housed post-operatively and allowed one week for recovery. On the day of an experiment, mice were brought from the vivarium to the testing room in their home cages and given 60 min for acclimation. In dose-response studies, mice received s.c. injections of a SCRA (0.001–30 mg/kg) or its vehicle and were subjected to a triad test procedure at 30 min intervals for 2 h. All SCRAs for in vivo studies were administered at a volume of 0.01 mL/g mouse body weight and dissolved in vehicle consisting of a 1:1:18 (v:v:v) ratio of DMSO, Tween 80, and saline, respectively. In antagonist reversal studies, mice received s.c. injections of either rimonabant (0.01–0.1 mg/kg) or vehicle (1:9 DMSO and saline) 30 min prior to administration of SCRAs and the triad test procedure at 30 min intervals for 2 h. We used a within-subjects design for the study, whereby cohorts of 15 mice were used to test dose-response and rimonabant pretreatment effects for each SCRA (90 total mice). Briefly, mice were tested once weekly for up to 6 weeks, and doses were randomized across test sessions.

The triad test procedure is an abbreviated version of the well-established tetrad test procedure [6, 39], which is routinely used to study the pharmacological effects of cannabinoids in rodents. The tetrad test measures locomotor activity, body temperature, catalepsy-like behavior, and analgesia. The triad test described here utilizes all measures of the tetrad test except assessment of locomotor activity. Elimination of locomotor testing allows for the repeated measurement of temperature, catalepsy, and analgesia in the same subject during a 2-h test session. Body temperature was measured non-invasively using a handheld reader that receives signals emitted from the surgically implanted temperature transponders. Catalepsy-like behavior was assessed next using the catalepsy bar test, similar to the method described in Metna-Laurent, et al. [39] with a 60 s cutoff time for maximum response. Briefly, the forelimbs of the mouse were placed onto the catalepsy bar and the latency to release the bar was recorded. Analgesia was measured last, as previously described in Metna-Laurent, et al. [39], using the hotplate test (IITC Life Sciences, Woodland Hills, CA, USA). Mice were placed onto a hot plate set at 52 °C and the latency to respond to the heat stimulus was recorded. Mice were immediately removed from the plate once they responded by jumping, flinching, or paw licking, and were returned to their home cages. A 45 s maximum cutoff time was used to prevent tissue damage. All 3 components of the triad were assessed in sequence every 30 min for 2 h post drug administration.

The raw temperature data for each mouse were transformed to temperature change from baseline in °C (i.e., temperature Δ) at each time point, to account for differences in baseline body temperature between mice. For the temperature dose-response and rimonabant analyses, mean temperature Δ across the 2-h session was calculated for each mouse. The raw catalepsy and hot plate data for each mouse were transformed to percent maximum possible effect (% MPE) at each time point, to normalize the differences in baseline responsiveness between mice: (experimental measure—baseline measure) / (maximum possible response—baseline measure) x 100. The maximum possible response for catalepsy latency was 60 s, whereas maximum possible response for hot plate latency was 45 s. For the catalepsy and analgesia dose-response and rimonabant results, mean %MPE across the 2-h session was calculated for each mouse.

Data analysis & statistics

All statistical analyses were performed using GraphPad Prism software (Prism Version 9, La Jolla, CA, USA). The effects of SCRAs on [^{3}H]rimonabant and [^{35}S]GTPγS binding were analyzed by non-linear regression. Data for these experiments were fit to the equation, $Y(x)=Ymin + (Ymax - Ymin) / (1 + 10exp[(logP50 - logx)] \times n)$, where x = concentration of compound tested, Y(x) = response measured, Ymax = maximal response, P50 = either IC_{50} or EC_{50}, and n = the Hill slope parameter. K_i was determined using the method of Cheng and Prusoff [42]. The time-course of drug effects on temperature Δ, catalepsy %MPE, and analgesia %MPE are shown for reference. The effect of drug dose on mean temperature Δ, catalepsy %MPE, and analgesia %MPE over the 2-h session was evaluated using the Kruskal-Wallis test, followed by Dunn's post hoc test to determine differences with respect to vehicle control. The effect of rimonabant pretreatment was evaluated using the Kruskal-Wallis test, followed by Dunn's post hoc test to determine differences with respect the vehicle/vehicle control group. ED_{50} values for mean cannabinoid-like effects over the 2-h session were determined using non-linear regression analyses. Relationships among K_i, EC_{50}, and ED_{50} values were analyzed by Spearman's correlation analysis. $p < 0.05$ was used as the minimum criterion for statistical significance in all cases.

RESULTS

5F-MDMB-PICA and its analogs are CB_1 agonists in vitro

Figure 2A depicts the effects of 5F-MDMB-PICA and its analogs on the binding of [^{3}H]rimonabant to CB_1 in mouse brain membranes. All of the SCRAs were fully efficacious inhibitors of [^{3}H]rimonabant binding. 5F-MDMB-PICA displayed the highest affinity for CB_1 (K_i = 1.24 nM), but there was a wide range of affinity values (K_i range of 1.24 to 263.3 nM) which are summarized in Table 1. The rank order of binding affinity at CB_1 was 5F-MDMB-PICA > AM-2201 ≈ 5F-CUMYL-PICA > 5F-NNEI ≈ 5F-MMB-PICA > 5F-SDB-006. It should be noted that the naturally occurring phytocannabinoid, THC, displayed a Ki = 43.31 nM in the binding assay, demonstrating that 5F-MDMB-PICA has ~35-fold higher affinity for mouse CB_1 when compared to THC. From a structure-activity perspective (see Fig. 1), changing the carbonyl linker of AM-2201 to the amide linker of 5F-NNEI induced a modest decrease in CB_1 binding affinity, whereas changing the naphthyl head group of 5F-NNEI to the benzyl head group of 5F-SDB-006 reduced affinity nearly 18-fold. The cumyl head group of 5F-CUMYL-PICA afforded CB_1 binding affinity that was similar to AM-2201. Finally, the 3,3-dimethylbutanoate head group of 5F-MDMB-PICA engendered 15-fold greater CB_1 binding affinity than the corresponding 3-methylbutanoate head group of 5F-MMB-PICA. The binding results demonstrate that subtle changes in head group composition can substantially influence CB_1 binding affinity for 5F-pentylindole SCRAs.

The [^{35}S]GTPγS binding assay provides an index of functional coupling between drug-receptor binding and its associated G protein-dependent intracellular signaling machinery. Here we used CP-55,940 as a standard full efficacy CB_1 agonist for comparison. Figure 2B shows the effects of 5F-MDMB-PICA and its analogs in the [^{35}S]GTPγS assay. All of the SCRAs exhibited agonist activity, and 5F-MDMB-PICA displayed the most potent actions for stimulating [^{35}S]GTPγS binding (EC_{50} = 1.46 nM; Table 1). All of the 5F-pentylindole SCRAs exerted maximal effects that ranged between 140 and 170% above baseline, which was similar to the effects of CP-55,940 (EC_{50} = 23.61 nM; E_{max} = 133%). 5F-SDB-006 had very weak potency in the [^{35}S]GTPγS assay when compared to the other 5F-pentylindole SCRAs. THC displayed low potency (EC_{50} = 186.01 nM) and low efficacy (41%) in the [^{35}S]

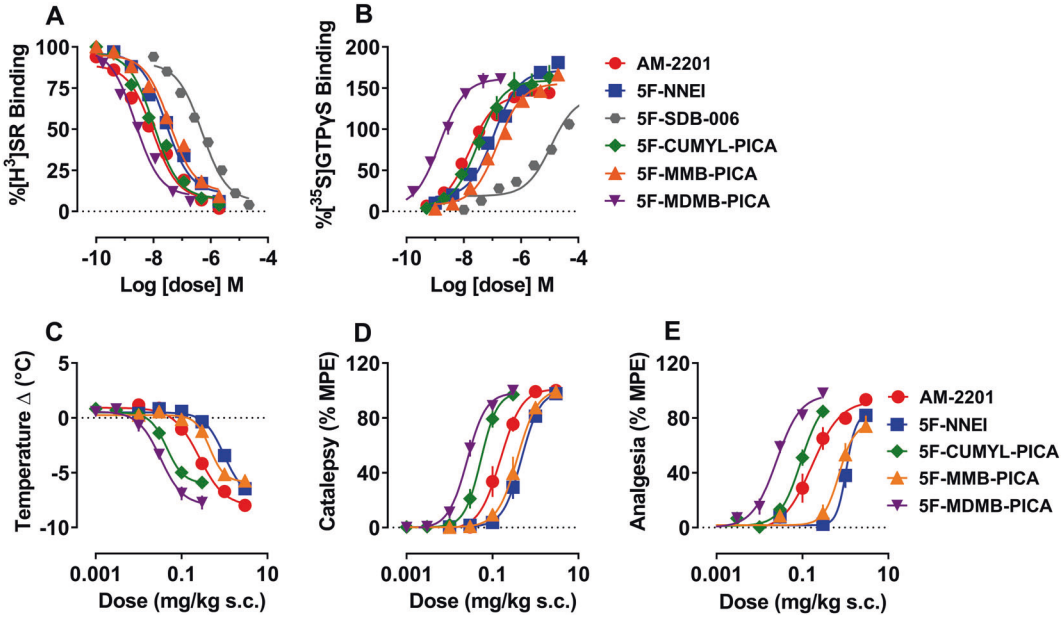

Fig. 2 Dose-response of 5F-MDMB-PICA and its analogs to compete for CB_1 binding, display CB_1 agonist effects, and produce cannabinoid-like effects in vivo. Concentration response curves for AM-2201 (red circles), 5F-NNEI (blue squares), 5F-SDB-006 (gray hexagons), 5F-CUMYL-PICA (green diamonds), 5F-MMB-PICA (orange upward triangles), and 5F-MDMB-PICA (purple downward triangles) to inhibit [^{3}H]rimonabant binding (**A**) and stimulate [^{35}S]GTPγS binding (**B**) in mouse brain membranes. Dose-response curves for effects of drugs on mean temperature change (Δ °C) (**C**), catalepsy expressed as percent maximum possible effect (%MPE) (**D**), and analgesia expressed as % MPE (**E**) in the triad test. In vitro data are mean ± SD for $n = 3$ separate experiments performed in triplicate, while in vivo data are mean ± SEM for $n = 7$–9 mice per dose. Affinity (K_i) and potency values (EC_{50}, ED_{50}) are found in Table 1.

Table 1. Affinity (K_i) and potency values (EC_{50}, ED_{50}) for 5F-MDMB-PICA and 5F-pentylindole analogs to exert cannabinoid-like effects.

Ligand	[^{3}H]Rimonabant Binding K_i (nM)	[^{35}S]GTPγS Assay EC_{50} (nM) [%Emax]	Temperature Δ °C ED_{50} (mg/kg)	Catalepsy %MPE ED_{50} (mg/kg)	Analgesia %MPE ED_{50} (mg/kg)
AM-2201	5.08 ± 0.91	16.31 ± 2.24 [142%]	0.25 ± 0.04	0.15 ± 0.02	0.16 ± 0.03
5F-NNEI	14.37 ± 5.28	114.51 ± 15.22 [171%]	1.01 ± 0.23	0.47 ± 0.05	1.06 ± 0.16
5F-SDB-006	263.3 ± 36.0	11,200 ± 2,653 [140%]	31.3 ± 15.0*	29.8 ± 4.35*	43.5 ± 6.69*
5F-CUMYL-PICA	5.48 ± 0.85	31.75 ± 6.90 [159%]	0.05 ± 0.01	0.05 ± 0.01	0.09 ± 0.01*
5F-MMB-PICA	19.51 ± 3.76	152.6 ± 20.1 [156%]	0.46 ± 0.07	0.38 ± 0.05	0.71 ± 0.12
5F-MDMB-PICA	1.24 ± 0.55	1.46 ± 0.19 [162%]	0.03 ± 0.01	0.03 ± 0.01	0.02 ± 0.01
THC	43.31 ± 6.47	186.01 ± 35.23 [41%]	n.d.	n.d.	n.d.

[^{3}H]Rimonabant binding assays and [^{35}S]GTPγS functional assays were carried out in mouse brain membranes as described in Materials and Methods. In vitro K_i and EC_{50} values are given in nM concentrations, expressed as mean ± SD for $n = 3$ experiments performed in triplicate. Assessments of mean temperature change (temperature Δ), catalepsy percent maximum possible effect (%MPE), and analgesia %MPE were carried out in male C57BL/6J mice as described in Materials and Methods. In vivo ED_{50} values are given as mg/kg, s.c., doses, expressed as mean ± SD for 7–9 mice per group. Asterisks indicate approximate potency values. n.d. = not determined.

GTPγS assay, consistent with its known low efficacy agonist actions. In general, the rank order of potencies in the [^{35}S]GTPγS assay mirrored the results of the [^{3}H]rimonabant binding assay, confirming a role of CB_1 agonism. However, the range of potency values in the [^{35}S]GTPγS assay was much greater than that observed for the receptor binding assay (EC_{50} range of 1.46 to 11,200 nM). As a specific example, in the [^{35}S]GTPγS assay, the 3,3-dimethylbutanoate head group of 5F-MDMB-PICA engendered ~100-fold greater potency than the corresponding 3-methylbutanoate head group of 5F-MMB-PICA (as compared to a 15-fold greater affinity in the binding assay). Overall, the findings with the [^{35}S]GTPγS assay suggest that subtle changes in head group composition of 5F-pentylindole SCRAs can alter functional potency at CB_1 much more than binding affinity.

5F-MDMB-PICA and its analogs induce cannabinoid-like effects in vivo

All of the SCRAs were tested for their ability to induce hypothermia, catalepsy, and analgesia in the mouse triad test procedure. Representative time-course data for the effects of 5F-MDMB-PICA in vivo are shown in Fig. 3A–C. The Kruskal-Wallis test revealed that 5F-MDMB-PICA administration significantly

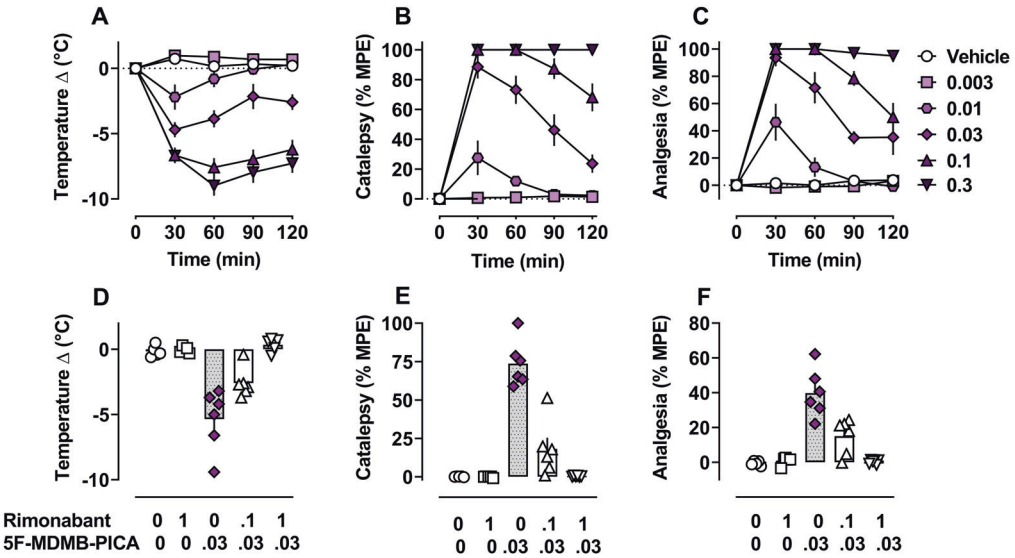

Fig. 3 Time-course and antagonist reversal of cannabinoid-like effects produced by 5F-MDMB-PICA. Effects of 0.003–0.3 mg/kg s.c. 5F-MDMB-PICA on temperature change (Δ °C) (**A**), catalepsy expressed as percent maximum possible effect (%MPE) (**B**), and analgesia expressed as %MPE (**C**) in the triad test, as assessed every 30 min over the 2 h testing period. Effect of rimonabant (0.1 or 1 mg/kg s.c.) pretreatment on mean temperature Δ (**D**), mean catalepsy %MPE (**E**), and mean analgesia %MPE (**F**) produced by 5F-MDMB-PICA. Data are expressed as mean ± SEM for $n = 8$–9 mice per dose in time-course plots and mean ± SEM for $n = 5$–6 mice per condition in antagonist reversal plots. **D**–**F** Filled bars & symbols represent statistically significant differences ($p < 0.05$) compared to the vehicle/vehicle control group.

impacted mean temperature Δ over the 2-h session ($H_{6,53} = 49.37$ $p < 0.0001$) (Figs. 2C and 3A). Dunn's test showed significant temperature reductions after the 0.1 mg/kg ($p = 0.0009$) and 0.3 mg/kg ($p = 0.0003$) doses, when compared to the vehicle control group. 5F-MDMB-PICA significantly affected mean catalepsy responses expressed as %MPE ($H_{6,53} = 55.60$ $p < 0.0001$; Figs. 2D and 3B), with significant increases above the control group for the 0.03 ($p = 0.0015$), 0.1 ($p = 0.0003$), and 0.3 mg/kg doses ($p < 0.0001$). In a similar manner, 5F-MDMB-PICA significantly affected mean analgesic responses expressed as %MPE ($H_{6,53} = 52.81$ $p < 0.0001$; Figs. 2E and 3C). In this case, significant analgesia was induced at 0.03 ($p = 0.0124$), 0.1 ($p < 0.0001$), and 0.3 ($p < 0.0001$) mg/kg doses. The time-course data depicted in Fig. 3A–C show that a dose of 0.01 mg/kg 5F-MDMB-PICA was the threshold dose required to induce changes in temperature, catalepsy, and analgesia, but the effects were transient and did not reach statistical significance when comparing mean effects over the 2-h session. Interestingly, the time-course data reveal that duration of drug action seemed to increase as dose administered increased from 0.01 to 0.3 mg/kg. At 0.3 mg/kg, 5F-MDMB-PICA caused reductions in body temperature that reached 8–9 °C below normal and evoked maximal effects on catalepsy and analgesia that lasted for the entire 2-h session. AM-2201, 5F-NNEI, 5F-SDB-006, 5F-CUMYL-PICA, 5F-MMB-PICA also produced dose-dependent effects in the triad test procedure, but most of the drugs required higher doses to elicit their effects when compared to 5F-MDMB-PICA (see Supplementary Figs. 1–5).

Mean effects on temperature Δ, catalepsy %MPE, and analgesia %MPE were used to construct dose-response curves and calculate ED_{50} potency values for all SCRAs tested (see Fig. 2C–E). As shown in Fig. 2C, 5F-MDMB-PICA and its analogs produced dose-dependent decreases in mean temperature Δ, but ED_{50} values for reducing body temperature varied across the drugs tested (Table 1). 5F-MDMB-PICA produced the most potent effects on hypothermia, while the effects of 5F-SDB-006 were much weaker than those of the other SCRAs tested (Supplementary Fig. 5A). With the exception of 5F-SDB-006, all of the drugs caused robust hypothermia, reaching 6–8 °C below normal. 5F-SDB-006 failed to produce reductions in temperature at any dose, though solubility issues prevented the testing of drug doses greater than 30 mg/kg. The rank order of potency for producing hypothermia was 5F-MDMB-PICA ≈ 5F-CUMYL-PICA > AM-2201 > 5F-MMB-PICA ≈ 5F-NNEI > 5F-SDB-006. Figure 2D demonstrates that SCRAs induced dose-dependent increases in mean catalepsy response expressed as %MPE. With the exception of 5F-SDB-006, which only reached ~50% of maximum (see Supplementary Fig. 5B), all of the drugs caused similar maximal effects on catalepsy (Fig. 2D). ED_{50} values for catalepsy varied across cannabinoids and the effect of 5F-SDB-006 was right shifted compared to effects of other 5F-pentylindoles (Table 1). 5F-MDMB-PICA produced the most potent effects on catalepsy. The rank order of potency for inducing catalepsy was 5F-MDMB-PICA ≈ 5F-CUMYL-PICA > AM-2201 > 5F-MMB-PICA ≈ 5F-NNEI > 5F-SDB-006. Figure 2E shows that all 5F-pentylindole SCRAs induced dose-dependent increases in mean analgesic response expressed as %MPE. All of the drugs produced potent and maximal effects, except for 5F-SDB-006 (Supplementary Fig. 5C). ED_{50} values for analgesia %MPE ranged from 0.02 to 44 mg/kg s.c., with 5F-MDMB-PICA producing the most potent effects (Table 1). Rank order of potency for analgesia was similar to that for catalepsy. It is noteworthy that 5F-CUMYL-PICA displayed slightly higher potency in vivo than would be expected from in vitro results, but otherwise the rank order was maintained between studies. Overall, the 5F-pentyindole SCRAs produce cannabinoid-like effects in mice, with 5F-MDMB-PICA displaying the highest potency for all measures of the triad test.

Effects of 5F-MDMB-PICA and its analogs are reversed by rimonabant

To assess the involvement of CB_1 in mediating the effects of 5F-pentylindole SCRAs in the triad test, we investigated effects of rimonabant pretreatment (0.1 and 1 mg/kg s.c.) 30 min prior to administration of 5F-MDMB-PICA or its analogs. Data for the effects of rimonabant pretreatment on responses induced by 5F-MDMB-PICA are shown in Fig. 3D–F. The Kruskal-Wallis test revealed that 5F-MDMB-PICA administration (0.03 mg/kg s.c.) produced effects on temperature Δ ($H_{4,23} = 21.72$ $p = 0.0002$) which were significant compared to the control group ($p = 0.0241$ versus vehicle/vehicle), and these effects were partially blocked by 0.1 mg/kg rimonabant and fully eliminated by 1.0 mg/kg rimonabant (*n.s.* versus vehicle/vehicle; Fig. 3D). In a similar manner, 5F-

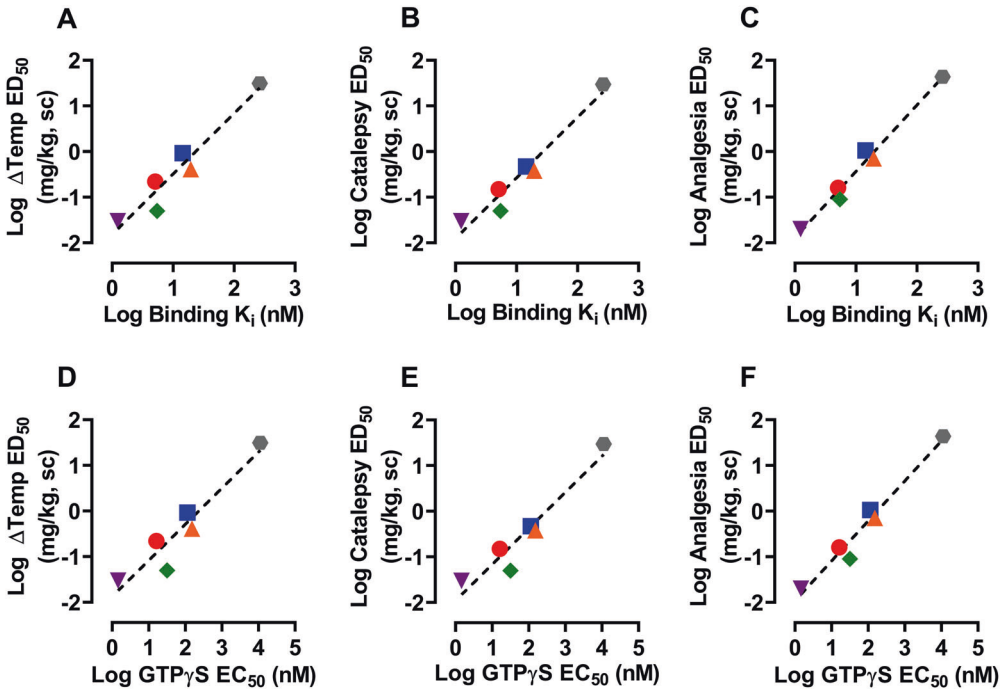

Fig. 4 Correlations between in vitro and in vivo CB_1 measures in mice. Relationships between in vitro affinities and potencies in mouse brain tissue and in vivo potencies for cannabinoid-like effects in mice determined in the triad test for AM-2201 (red circles), 5F-NNEI (blue squares), 5F-SDB-006 (gray octagons), 5F-CUMYL-PICA (green diamonds), 5F-MMB-PICA (orange upward triangles), and 5F-MDMB-PICA (purple downward triangles). Spearman rank correlations between log K_i for binding in vitro and in vivo log ED_{50} parameters of the triad test (**A**–**C**). Spearman rank correlations between log EC_{50} for efficacy in vitro and in vivo log ED_{50} parameters of the triad test (**E**–**F**).

MDMB-PICA induced effects on mean catalepsy %MPE ($H_{4,23} = 22.32$ $p = 0.0002$) and mean analgesia %MPE ($H_{4,23} = 19.91$ $p = 0.0002$), that were partially blocked by 0.1 mg/kg rimonabant pretreatment and fully eliminated by 1 mg/kg rimonabant pretreatment (*n.s.* versus vehicle/vehicle; Fig. 3E-F). The effects of AM-2201 (0.3 mg/kg, s.c.), 5F-NNEI (1 mg/kg, s.c.), 5F-CUMYL-PICA (0.1 mg/kg s.c.), and 5F-MMB-PICA (1 mg/kg s.c.) were also partially blocked by 0.1 mg/kg rimonabant pretreatment and fully eliminated (*n.s.* versus vehicle/vehicle) by 1 mg/kg rimonabant pretreatment (see Supplementary Figs. 1–4).

K_i and EC_{50} values predict in vivo potency

To assess the relationships between in vitro measures and in vivo potency in triad assessments, we carried out Spearman rank correlation analyses using K_i, EC_{50}, and ED_{50} values reported in Table 1. Binding affinity (K_i) values displayed significant positive correlations with in vivo ED_{50} estimates for temperature, catalepsy, and analgesia ($r = 0.89$ $p = 0.03$, for all endpoints) measured in the triad test (Fig. 4A–C). Similarly, functional EC_{50} values exhibited significant positive correlations with in vivo ED_{50} estimates for temperature, catalepsy, and analgesia ($r = 0.89$ $p = 0.03$, for all endpoints) measured in the triad test (Fig. 4D–F). These results demonstrate a strong relationship between in vitro K_i and EC_{50} values in mouse brain and in vivo measures in the triad test of cannabinoid-like activity in mice.

DISCUSSION

A major aim of the present study was to characterize the in vitro and in vivo pharmacology of the synthetic cannabinoid 5F-MDMB-PICA in mice. 5F-MDMB-PICA is a problematic drug of abuse associated with serious medical complications, including erratic behavior, aggression, disorientation, and coma [27]. In addition, we sought to compare the effects of 5F-MDMB-PICA to a number of structurally related 5F-pentylindole analogs that vary only in their head group composition (see Fig. 1). Our investigation revealed four key findings: (1) 5F-MDMB-PICA is a potent and efficacious CB_1 agonist in mouse brain tissue, in agreement with data from cells transfected with human CB_1 [22, 31–33] as well as data from rat cerebellar membranes [30]; (2) 5F-MDMB-PICA induces dose- and time-dependent hypothermia, catalepsy, and analgesia in vivo, consistent with the effects of other indole-containing SCRAs in rodents [43–47]; (3) Altering head group composition of 5F-pentylindoles dramatically affects CB_1 activity, whereby 3,3-dimethylbutanoate (i.e., 5F-MDMB-PICA) and cumyl (i.e., 5F-CUMYL-PICA) groups engender high potency while a benzyl group engenders low potency [7, 8]; (4) In vitro K_i affinity and EC_{50} potency values at CB_1 display strong positive correlations with in vivo potency of the 5F-pentylindole analogs examined here. Overall, our results demonstrate that CB_1 affinity and potency determinations in mouse brain tissue are predictive of cannabinoid-like effects in this species and support the known utility of mouse models for characterizing the pharmacological effects of emerging SCRAs.

As far as we are aware, only one published study has examined the affinity of 5F-MDMB-PICA at CB_1 in native tissue preparations, where the drug had an $IC_{50} = 2.0$ nM in rat cerebellar membranes [30]. Here, we show that 5F-MDMB-PICA displays high affinity for [^{3}H]rimonabant-labeled CB_1 in mouse brain membranes ($K_i = 1.24$ nM) when compared to the effects of other 5F-pentylindole SCRAs. Under identical binding assay conditions, THC has a $K_i = 43.3$ nM at CB_1, indicating 5F-MDMB-PICA displays ~35-fold higher affinity than THC for [^{3}H]rimonabant-labeled sites (Table 1). In our binding assay, the comparator drug AM-2201 has a $K_i = 5.08$ nM at CB_1, an affinity that is somewhat weaker than the CB_1 affinity reported by others [48, 49]. However, it is important to note that previous studies examining AM-2201 binding in brain tissue employed the CB_1 agonist radioligand [^{3}H]CP-55,940 whereas we used the CB_1 antagonist radioligand [^{3}H]rimonabant. Here we report a $K_i = 5.48$ nM for 5F-CUMYL-PICA at mouse CB_1, which

agrees well with data from Banister, et al. [50] who examined the effects of 5F-CUMYL-PICA on [^{3}H]rimonabant binding to human CB_1 expressed in human embryonic kidney 293 (HEK293) cells. In general, the limited CB_1 binding data available for emerging SCRAs suggest that drug affinities for [^{3}H]rimonabant binding in mouse brain membranes are similar to those reported for [^{3}H]rimonabant binding in cells expressing human CB_1.

A number of prior studies have examined the functional activity of 5F-MDMB-PICA in heterologous cells transfected with CB_1 [22, 31–33], but our results from the [^{35}S]GTPγS assay represent the first examination of functional activity at CB_1 for the compound in a native tissue preparation. We found that 5F-MDMB-PICA displays the most potent agonist activity at CB_1 in mouse brain membranes ($EC_{50} = 1.46$ nM) when compared to the effects of other 5F-pentylindole SCRAs. 5F-MDMB-PICA and its analogs exhibit agonist actions to stimulate [^{35}S]GTPγS binding, with E_{max} values mirroring that of the prototypical full-efficacy cannabinoid agonist CP-55,940 ($EC_{50} = 23.6$ nM, $E_{max} = 133\%$; Table 1). In general, our results for 5F-MDMB-PICA in the [^{35}S]GTPγS assay are consistent with findings from functional assays carried out in other laboratories. These prior studies show that 5F-MDMB-PICA has sub to low nM agonist potency in CB_1-transfected cells, but EC_{50} potency values varied from 0.45 to 27.6 nM. The reported differences in agonist potency for 5F-MDMB-PICA across previous studies likely reflects the unique in vitro bioassay methods used by each laboratory as well as differences in reference compounds used for comparison.

A critical goal of our study was to characterize structure-activity relationships (SAR) for analogs of 5F-MDMB-PICA that varied only in their head group composition. A number of investigations by Banister and colleagues [7, 8, 22, 32, 51, 52] have examined in vitro functional potencies (i.e., EC_{50} values) for structurally related SCRAs by using a fluorescence-based membrane potential bioassay in cells transfected with either human CB_1 or CB_2. With respect to the present work, Banister & colleagues have shown that 5F-MDMB-PICA and 5F-MMB-PICA display EC_{50} values of 0.45 and 2.4 nM at CB_1, respectively. Our data from the [^{35}S]GTPγS assay in mouse brain membranes generally agree that the additional methyl group of 5F-MDMB-PICA increases functional potency at CB_1 when compared to 5F-MMB-PICA, but we found much greater enhancement of potency where 5F-MDMB-PICA ($EC_{50} = 1.46$ nM) is 100-fold more potent than 5F-MMB-PICA ($EC_{50} = 152.6$ nM). Perhaps the most dramatic effect of head group composition that we observed was the comparison of the cumyl head group in 5F-CUMYL-PICA and the benzyl head group in 5F-SDB-006. In this case, we show that addition of a dimethyl group enhances functional potency of 5F-CUMYL-PICA ($EC_{50} = 31.75$ nM) more than 300-fold versus 5F-SDB-006 ($EC_{50} = 11{,}200$ nM). Importantly, Ametovski, et al. [52] recently reported that 5F-CUMYL-PICA displays much greater affinity and potency than 5F-SDB-006, when tested in cells transfected with human CB_1. Together with the existing SAR findings from transfected cells, the present data using GTPγS binding in mouse brain membranes confirm that head group composition can dramatically influence CB_1 functional activation, where the strategic placement of methyl groups can substantially enhance drug potency. Our SAR findings may have important implications for predicting the risk of cannabinoid NPS as they emerge in clandestine drug markets.

Despite the widespread misuse of 5F-MDMB-PICA, little information is available about the in vivo effects of the drug in animal models. Krotulski et al. recently reported that administration of 0.05–0.2 mg/kg 5F-MDMB-PICA to rats produces robust hypothermia and catalepsy lasting for up to 4 h [30]. In agreement with the rat data, we show that 5F-MDMB-PICA induces cannabinoid-like effects in mice, including hypothermia, catalepsy, and analgesia. The effects elicited by 5F-MDMB-PICA are consistent with those reported for other SCRAs in rodent models [43–47], but 5F-MDMB-PICA is especially potent. We show that 0.01 mg/kg, s.c., is the threshold dose for inducing cannabinoid-like effects in mice, and a tenfold higher dose produces robust and sustained effects that last for at least 2 h after injection. Notably, the effects of 5F-MDMB-PICA are completely reversed by rimonabant pretreatment, confirming the critical role of CB_1. The high in vivo potency of 5F-MDMB-PICA shown here in mice is consistent with the powerful effects of the drug reported in humans, often leading to serious intoxication, overdose, and even death [27, 28]. It seems unlikely that the effects of 5F-MDMB-PICA in mice can fully recapitulate the complex toxicological effects reported in human users, but severe hypothermia has been reported in some patients intoxicated with SCRAs [53, 54]. Only one other study has examined in vivo effects of 5F-MDMB-PICA in mice [55]. Musa, et al. [55] examined the neurochemical actions of 5F-MDMB-PICA on extracellular dopamine concentrations in mouse nucleus accumbens shell. These investigators observed that 0.01 mg/kg, i.p., 5F-MDMB-PICA significantly increases extracellular dopamine concentrations in adolescent but not adult animals [55]. In the same study, when mice were treated during adolescence for 2 weeks with 5F-MDMB-PICA and tested for behavioral effects in adulthood, the mice displayed anxiety-like behavior in the marble burying test. The findings of Musa et al. suggest that in addition to potent cannabinoid-like effects reported here, 5F-MDMB-PICA may produce rewarding and anxiety-like effects. It is important to mention that our in vivo tests were confined to male mice. Given the emerging literature on sex differences in the effects of THC [56–59], future studies should assess possible sex differences in the behavioral effects of 5F-MDMB-PICA and other emerging SCRAs. Collectively, the in vivo effects reported for 5F-MDMB-PICA in animals may help to explain the potent subjective and pharmacological effects of 5F-MDMB-PICA and related SCRAs in humans, when compared to effects of cannabis or THC-based products.

Because we tested in vitro and in vivo effects of 5F-MDMB-PICA and its analogs in the same species, we sought to examine the relationships among K_i, EC_{50}, and ED_{50} values obtained for the compounds. In short, we wished to assess whether in vitro activity at CB_1 could predict in vivo potency of the SCRAs tested, as suggested by others [35–37]. Here we demonstrate significant positive correlations between in vitro K_i values for affinity at CB_1 and in vivo potencies for induction of cannabinoid-like effects in the mouse triad test. Significant positive correlations were similarly found when examining EC_{50} values for stimulation of GTPγS binding and in vivo ED_{50} values from triad experiments. Our findings agree with previous work of other groups who have demonstrated that affinity at human CB_1 or rat CB_1 is predictive of in vivo potency of various SCRAs and other cannabinoids in mice and rats [35–37]. Importantly, the behavioral potencies of cannabinoids in rodents seem to predict potencies for behavioral effects in humans [34, 35]. In contrast to our results, Marusich, et al. [37] only found significant positive correlations between affinity of SCRAs at human CB_1 and potency in mouse drug discrimination studies, but not potency for GTPγS binding at human CB_1. The use of cell membrane preparations transfected with human CB_1 versus membranes isolated from mouse brain tissue in the present study may explain this discrepancy.

The in vivo potencies for 5F-pentylindole cannabinoid compounds in rodents appear to be quite similar across different studies. For example, we show that 5F-CUMYL-PICA induces hypothermia, catalepsy, and analgesia with ED_{50} values ranging from 0.05 to 0.09 mg/kg, s.c., and Gamage et al. reported 5F-CUMYL-PICA has an ED_{50} of 0.05 mg/kg for THC-appropriate responding in a mouse drug discrimination paradigm. Likewise, we show that AM-2201 induces cannabinoid-like effects with ED_{50} values ranging from 0.15 to 0.25 mg/kg, s.c., while Gatch and Forster [60] showed AM-2201 has an ED_{50} of 0.11 mg/kg, i.p., for eliciting THC-appropriate responding in a rat drug discrimination assay. Available evidence demonstrates that testing the effects of

SCRAs in rodents may yield more reproducible findings across laboratories when compared to the effects from in vitro bioassays in transfected cells. Future studies should examine CB_1 affinities, potencies, and in vivo activities for a wider variety of SCRAs, to further evaluate the utility of using mice to study the pharmacology of emerging SCRAs.

To summarize, we show that 5F-MDMB-PICA is a potent and efficacious CB_1 agonist in vitro and in vivo. In addition, we demonstrate that head group composition of 5F-pentylindole SCRAs is a critical determinant governing cannabinoid effects, whereby 3,3-dimethylbutanoate and cumyl head groups engender potent CB_1 activity. 5F-MDMB-PICA continues to be a widely abused SCRA, despite being banned by drug control legislation in many parts of the world, and analogs of the compound are appearing as problematic NPS (e.g., 4F-MDMB-BICA & MDMB-4en-PINACA) [61–67]. As such, reliable methods for rapidly characterizing the pharmacological effects of the vast number of emerging SCRAs are needed. We show here that potency of 5F-pentylindole SCRAs at CB_1 in mouse brain tissue is highly correlated with cannabinoid-like effects in the triad test. Our findings indicate that in vitro assays using mouse brain membranes and in vivo methods using a triad procedure in mice can be useful screening tools to study the pharmacology of emerging SCRAs and can complement the in vitro data derived from assays carried out in cells transfected with human CB_1.

REFERENCES

1. Luethi D, Liechti ME. Designer drugs: mechanism of action and adverse effects. Arch Toxicol. 2020;94:1085–133.
2. Baumann MH, Solis E Jr., Watterson LR, Marusich JA, Fantegrossi WE, Wiley JL. Baths salts, spice, and related designer drugs: the science behind the headlines. J Neurosci. 2014;34:15150–8.
3. UNODC. United Nations Office on Drugs and Crime Early Warning Advisory Current NPS Threats - Volume III. 2020. https://www.unodc.org/documents/scientific/Current_NPS_Threats_Vol.4.pdf.
4. Banister SD, Arnold JC, Connor M, Glass M, McGregor IS. Dark classics in chemical neuroscience: δ(9)-tetrahydrocannabinol. ACS Chem Neurosci. 2019;10:2160–75.
5. Worob A, Wenthur C. DARK classics in chemical neuroscience: synthetic cannabinoids (Spice/K2). ACS Chem Neurosci. 2020;11:3881–92.
6. Wiley JL, Marusich JA, Thomas BF. Combination chemistry: structure-activity relationships of novel psychoactive cannabinoids. Curr Top Behav Neurosci. 2017;32:231–48.
7. Banister SD, Connor M. The chemistry and pharmacology of synthetic cannabinoid receptor agonist new psychoactive substances: evolution. Handb Exp Pharmacol. 2018;252:191–226.
8. Banister SD, Connor M. The chemistry and pharmacology of synthetic cannabinoid receptor agonists as new psychoactive substances: origins. Handb Exp Pharmacol. 2018;252:165–90.
9. Kraemer M, Boehmer A, Madea B, Maas A. Death cases involving certain new psychoactive substances: a review of the literature. Forensic Sci Int. 2019;298:186–267.
10. Wiley JL, Lefever TW, Marusich JA, Craft RM. Comparison of the discriminative stimulus and response rate effects of (Δ9)-tetrahydrocannabinol and synthetic cannabinoids in female and male rats. Drug Alcohol Depend. 2017;172:51–59.
11. Hoffman AF, Lycas MD, Kaczmarzyk, Spivak CE, Baumann MH, Lupica CR. Disruption of hippocampal synaptic transmission and long-term potentiation by psychoactive synthetic cannabinoid 'Spice' compounds: comparison with Δ^9-tetrahydrocannabinol. Addict Biol. 2017;22:390–9.
12. Yano H, Adhikari P, Naing S, Hoffman AF, Baumann MH, Lupica CR, et al. Positive allosteric modulation of the 5-HT(1A) receptor by indole-based synthetic cannabinoids abused by humans. ACS Chem Neurosci. 2020;11:1400–05.
13. Patel M, Manning JJ, Finlay DB, Javitch JA, Banister SD, Grimsey NL, et al. Signalling profiles of a structurally diverse panel of synthetic cannabinoid receptor agonists. Biochem Pharmacol. 2020;175:113871.
14. Wouters E, Walraed J, Banister SD, Stove CP. Insights into biased signaling at cannabinoid receptors: synthetic cannabinoid receptor agonists. Biochem Pharmacol. 2019;169:113623.
15. Mogler L, Franz F, Rentsch D, Angerer V, Weinfurtner G, Longworth M, et al. Detection of the recently emerged synthetic cannabinoid 5F-MDMB-PICA in 'legal high' products and human urine samples. Drug Test Anal. 2018;10:196–205.
16. Ong RS, Kappatos DC, Russell SGG, Poulsen HA, Banister SD, Gerona RR, et al. Simultaneous analysis of 29 synthetic cannabinoids and metabolites, amphetamines, and cannabinoids in human whole blood by liquid chromatography-tandem mass spectrometry—A New Zealand perspective of use in 2018. Drug Test Anal. 2020;12:195–214.
17. Krotulski AJ, Mohr ALA, Logan BK. Emerging synthetic cannabinoids: development and validation of a novel liquid chromatography quadrupole time-of-flight mass spectrometry assay for real-time detection. J Anal Toxicol. 2020;44:207–17.
18. Krotulski AJ, Mohr ALA, Logan BK Synthetic Cannabinoids in the United States - Trend Report: Q3 2020. CFSRE NPS Discovery Public Health Alert. 2020.
19. Krotulski AJ, Mohr ALA, Logan BK Synthetic Cannabinoids in the United States - Trend Report: Q2 2020. CFSRE NPS Discovery Public Health Alert. 2020.
20. Krotulski AJ, Mohr ALA, Logan BK Synthetic Cannabinoids in the United States - Trend Report: Q1 2020. CFSRE NPS Discovery Public Health Alert. 2020.
21. Krotulski AJ, Walton SE, Mohr ALA, Logan BK Synthetic Cannabinoids in the United States - Trend Report: Q4 2020. CFSRE NPS Discovery Public Health Alert. 2021.
22. Banister SD, Longworth M, Kevin R, Sachdev S, Santiago M, Stuart J, et al. Pharmacology of valinate and tert-leucinate synthetic cannabinoids 5F-AMBICA, 5F-AMB, 5F-ADB, AMB-FUBINACA, MDMB-FUBINACA, MDMB-CHMICA, and Their Analogues. ACS Chem Neurosci. 2016;7:1241–54.
23. Risseeuw MDP, Blanckaert P, Coopman V, Van Quekelberghe S, Van Calenbergh S, Cordonnier J. Identification of a newtert-leucinate class synthetic cannabinoid in powder and "spice-like" herbalincenses: Methyl2-[[1-(5-fluoropentyl)indole-3-carbonyl]amino]-3,3-dimethyl-butanoate(5F-MDMB-PICA). Forensic Sci Int.2017;273:45–52.
24. Krotulski AJ, Bishop-Freeman SC, Mohr ALA, Logan BK. Evaluation of synthetic cannabinoid metabolites in human blood in the absence of parent compounds: a stability assessment. J Anal Toxicol. 2021;45:60–68.
25. Norman C, Walker G, McKirdy B, McDonald C, Fletcher D, Antonides LH, et al. Detection and quantitation of synthetic cannabinoid receptor agonists in infused papers from prisons in a constantly evolving illicit market. Drug Test Anal. 2020;12:538–54.
26. Antonides LH, Cannaert A, Norman C, NicDaeid N, Sutcliffe OB, Stove CP, et al. Shape matters: The application of activity-based in vitro bioassays and chiral profiling to the pharmacological evaluation of synthetic cannabinoid receptor agonists in drug-infused papers seized in prisons. Drug Test Anal. 2021;13:628–43.
27. Kleis J, Germerott T, Halter S, Héroux V, Roehrich J, Schwarz CS, et al. The synthetic cannabinoid 5F-MDMB-PICA: a case series. Forensic Sci Int. 2020;314:110410.
28. Shi Y, Zhou L, Li L, Liu M, Qiang H, Shen M, et al. Detection of a new tert-leucinate synthetic cannabinoid 5F-MDMB-PICA and its metabolites in human hair: application to authentic cases. Front Chem. 2020;8:610312.
29. DEA. Schedules of Controlled Substances: Temporary Placement of 5F-EDMB-PINACA, 5F-MDMB-PICA, FUB-AKB48, 5F-CUMYL-PINACA, and FUB-144 into Schedule I. Federal Register. 2019;84 FR 15505:15505-11.
30. Krotulski AJ, Garibay N, Walther D, Walton SE, Mohr ALA, Logan BK, et al. Pharmacokinetics and pharmacodynamics of the synthetic cannabinoid, 5F-MDMB-PICA, in male rats. Neuropharmacology. 2021;199:108800.
31. Noble C, Cannaert A, Linnet K, Stove CP. Application of an activity-based receptor bioassay to investigate the in vitro activity of selected indole- and indazole-3-carboxamide-based synthetic cannabinoids at CB1 and CB2 receptors. Drug Test Anal. 2019;11:501–11.
32. Sachdev S, Vemuri K, Banister SD, Longworth M, Kassiou M, Santiago M, et al. In vitro determination of the efficacy of illicit synthetic cannabinoids at CB(1) receptors. Br J Pharmacol. 2019;176:4653–65.
33. Truver MT, Watanabe S, Åstrand A, Vikingsson S, Green H, Swortwood MJ, et al. 5F-MDMB-PICA metabolite identification and cannabinoid receptor activity. Drug Test Anal. 2020;12:127–35.
34. Balster RL, Prescott WR. Δ9-Tetrahydrocannabinol discrimination in rats as a model for cannabis intoxication. Neurosci Biobehav Rev. 1992;16:55–62.
35. Compton DR, Rice KC, De Costa BR, Razdan RK, Melvin LS, Johnson MR, et al. Cannabinoid structure-activity relationships: correlation of receptor binding and in vivo activities. J Pharm Exp Ther. 1993;265:218–26.
36. Gamage TF, Farquhar CE, Lefever TW, Marusich JA, Kevin RC, McGregor IS, et al. Molecular and behavioral pharmacological characterization of abused synthetic cannabinoids MMB- and MDMB-FUBINACA, MN-18, NNEI, CUMYL-PICA, and 5-Fluoro-CUMYL-PICA. J Pharm Exp Ther. 2018;365:437–46.
37. Marusich JA, Wiley JL, Lefever TW, Patel PR, Thomas BF. Finding order in chemical chaos—Continuing characterization of synthetic cannabinoid receptor agonists. Neuropharmacology. 2018;134:73–81.
38. Porcu A, Melis M, Turecek R, Ullrich C, Mocci I, Bettler B, et al. Rimonabant, a potent CB1 cannabinoid receptor antagonist, is a Gαi/o protein inhibitor. Neuropharmacology. 2018;133:107–20.

39. Metna-Laurent M, Mondésir M, Grel A, Vallée M, Piazza PV. Cannabinoid-induced tetrad in mice. Curr Protoc Neurosci. 2017;80:9.59.1–9.59.10.
40. Dhopeshwarkar AS, Nicholson RA. Benzophenanthridine alkaloid, piperonyl butoxide and (S)-methoprene action at the cannabinoid-1 receptor (CB1-receptor) pathway of mouse brain: Interference with [3H]CP55940 and [3H]SR141716A binding and modification of WIN55212-2-dependent inhibition of synaptosomal l-glutamate release. Eur J Pharmacol. 2014;723:431–41.
41. De Luca MA, Castelli MP, Loi B, Porcu A, Martorelli M, Miliano C, et al. Native CB1 receptor affinity, intrinsic activity and accumbens shell dopamine stimulant properties of third generation SPICE/K2 cannabinoids: BB-22, 5F-PB-22, 5F-AKB-48 and STS-135. Neuropharmacology. 2016;105:630–38.
42. Cheng Y, Prusoff WH. Relationship between the inhibition constant (K1) and the concentration of inhibitor which causes 50 per cent inhibition (I50) of an enzymatic reaction. Biochem Pharmacol. 1973;22:3099–108.
43. Wiley JL, Marusich JA, Huffman JW. Moving around the molecule: relationship between chemical structure and in vivo activity of synthetic cannabinoids. Life Sci. 2014;97:55–63.
44. Ossato A, Canazza I, Trapella C, Vincenzi F, De Luca MA, Rimondo C, et al. Effect of JWH-250, JWH-073 and their interaction on "tetrad", sensorimotor, neurological and neurochemical responses in mice. Prog Neuropsychopharmacol Biol Psychiatry. 2016;67:31–50.
45. Wang XF, Galaj E, Bi GH, Zhang C, He Y, Zhan J, et al. Different receptor mechanisms underlying phytocannabinoid- versus synthetic cannabinoid-induced tetrad effects: Opposite roles of CB(1) /CB(2) versus GPR55 receptors. Br J Pharmacol. 2020;177:1865–80.
46. Schindler CW, Gramling BR, Justinova Z, Thorndike EB, Baumann MH. Synthetic cannabinoids found in "spice" products alter body temperature and cardiovascular parameters in conscious male rats. Drug Alcohol Depend. 2017;179:387–94.
47. Carlier J, Wohlfarth A, Salmeron BD, Scheidweiler KB, Huestis MA, Baumann MH. Pharmacodynamic effects, pharmacokinetics, and metabolism of the synthetic cannabinoid AM-2201 in male rats. J Pharm Exp Ther. 2018;367:543–50.
48. Chimalakonda KC, Seely KA, Bratton SM, Brents LK, Moran CL, Endres GW, et al. Cytochrome P450-mediated oxidative metabolism of abused synthetic cannabinoids found in K2/Spice: identification of novel cannabinoid receptor ligands. Drug Metab Dispos. 2012;40:2174–84.
49. Makriyannis A, Deng H Cannabimimetic indole derivatives. US patent 6,900,236 B1. 2005.
50. Banister SD, Adams A, Kevin RC, Macdonald C, Glass M, Boyd R, et al. Synthesis and pharmacology of new psychoactive substance 5F-CUMYL-P7AICA, a scaffold-hopping analog of synthetic cannabinoid receptor agonists 5F-CUMYL-PICA and 5F-CUMYL-PINACA. Drug Test Anal. 2019;11:279–91.
51. Longworth M, Banister SD, Boyd R, Kevin RC, Connor M, McGregor IS, et al. Pharmacology of cumyl-carboxamide synthetic cannabinoid new psychoactive substances (NPS) CUMYL-BICA, CUMYL-PICA, CUMYL-5F-PICA, CUMYL-5F-PINACA, and their analogues. ACS Chem Neurosci. 2017;8:2159–67.
52. Ametovski A, Macdonald C, Manning JJ, Haneef SAS, Santiago M, Martin L, et al. Exploring stereochemical and conformational requirements at cannabinoid receptors for synthetic cannabinoids related to SDB-006, 5F-SDB-006, CUMYL-PICA, and 5F-CUMYL-PICA. ACS Chem Neurosci. 2020;11:3672–82.
53. Nacca N, Schult R, Loflin R, Weltler A, Gorodetsky R, Kacinko S, et al. Coma, seizures, atrioventricular block, and hypoglycemia in an ADB-FUBINACA body-packer. J Emerg Med. 2018;55:788–91.
54. Seywright A, Torrance HJ, Wylie FM, McKeown DA, Lowe DJ, Stevenson R. Analysis and clinical findings of cases positive for the novel synthetic cannabinoid receptor agonist MDMB-CHMICA. Clin Toxicol (Philos). 2016;54:632–7.
55. Musa A, Simola N, Piras G, Caria F, Onaivi ES, De Luca MA Neurochemical and behavioral characterization after acute and repeated exposure to novel synthetic cannabinoid agonist 5-MDMB-PICA. Brain Sci. 2020;10:1011.
56. Moore CF, Davis CM, Harvey EL, Taffe MA, Weerts EM. Appetitive, antinociceptive, and hypothermic effects of vaped and injected Δ-9-tetrahydrocannabinol (THC) in rats: exposure and dose-effect comparisons by strain and sex. Pharmacol Biochem Behav. 2021;202:173116.
57. Javadi-Paydar M, Nguyen JD, Kerr TM, Grant Y, Vandewater SA, Cole M, et al. Effects of Δ9-THC and cannabidiol vapor inhalation in male and female rats. Psychopharmacol. 2018;235:2541–57.
58. Nguyen JD, Aarde SM, Vandewater SA, Grant Y, Stouffer DG, Parsons LH, et al. Inhaled delivery of Δ9-tetrahydrocannabinol (THC) to rats by e-cigarette vapor technology. Neuropharmacology. 2016;109:112–20.
59. Nguyen JD, Creehan KM, Grant Y, Vandewater SA, Kerr TM, Taffe MA. Explication of CB(1) receptor contributions to the hypothermic effects of Δ(9)-tetrahydrocannabinol (THC) when delivered by vapor inhalation or parenteral injection in rats. Drug Alcohol Depend. 2020;214:108166.
60. Gatch MB, Forster MJ. Δ9-Tetrahydrocannabinol-like discriminative stimulus effects of compounds commonly found in K2/Spice. Behav Pharmacol. 2014;25:750–7.
61. Krotulski AJ, Walton SE, Mohr ALA, Logan BK Synthetic Cannabinoids in the United States - Trend Report: Q1 2021. CFSRE NPS Discovery Public Health Alert. 2021.
62. Cannaert A, Sparkes E, Pike E, Luo JL, Fang A, Kevin RC, et al. Synthesis and in vitro cannabinoid receptor 1 activity of recently detected synthetic cannabinoids 4F-MDMB-BICA, 5F-MPP-PICA, MMB-4en-PICA, CUMYL-CBMICA, ADB-BINACA, APP-BINACA, 4F-MDMB-BINACA, MDMB-4en-PINACA, A-CHMINACA, 5F-AB-P7AICA, 5F-MDMB-P7AICA, and 5F-AP7AICA. ACS Chem Neurosci. 2020;11:4434–46.
63. Grafinger KE, Cannaert A, Ametovski A, Sparkes E, Cairns E, Banister SD, et al. Systematic evaluation of a panel of 30 synthetic cannabinoid receptor agonists structurally related to MMB-4en-PICA, MDMB-4en-PINACA, ADB-4en-PINACA, and MMB-4CN-BUTINACA using a combination of binding and different CB(1) receptor activation assays-Part II: Structure activity relationship assessment via a β-arrestin recruitment assay. Drug Test Anal. 2021;13:1402–11.
64. Grafinger KE, Vandeputte MM, Cannaert A, Ametovski A, Sparkes E, Cairns E, et al. Systematic evaluation of a panel of 30 synthetic cannabinoid receptor agonists structurally related to MMB-4en-PICA, MDMB-4en-PINACA, ADB-4en-PINACA, and MMB-4CN-BUTINACA using a combination of binding and different CB1 receptor activation assays. Part III: The G protein pathway and critical comparison of different assays. Drug Test Anal. 2021;13:1412–29.
65. Krotulski AJ, Cannaert A, Stove C, Logan BK. The next generation of synthetic cannabinoids: Detection, activity, and potential toxicity of pent-4en and but-3en analogues including MDMB-4en-PINACA. Drug Test Anal. 2021;13:427–38.
66. Norman C, Halter S, Haschimi B, Acreman D, Smith J, Krotulski AJ, et al. A transnational perspective on the evolution of the synthetic cannabinoid receptor agonists market: Comparing prison and general populations. Drug Test Anal. 2021;13:841–52.
67. Pike E, Grafinger KE, Cannaert A, Ametovski A, Luo JL, Sparkes E, et al. Systematic evaluation of a panel of 30 synthetic cannabinoid receptor agonists structurally related to MMB-4en-PICA, MDMB-4en-PINACA, ADB-4en-PINACA, and MMB-4CN-BUTINACA using a combination of binding and different CB(1) receptor activation assays: Part I-Synthesis, analytical characterization, and binding affinity for human CB(1) receptors. Drug Test Anal. 2021;13:1383–401.

ACKNOWLEDGEMENTS

We would like to thank Harvey Motulsky Ph.D., David Epstein Ph.D., Leigh Panlilio, Ph.D., and Yavin Shaham Ph.D. for their helpful feedback regarding statistical analyses employed in this manuscript.

AUTHOR CONTRIBUTIONS

GCG conducted in vivo triad experiments and wrote the manuscript. JSP conducted in vitro competition binding experiments and efficacy experiments. MHB designed the experiments, assisted with data interpretation, and revised the manuscript.

FUNDING INFORMATION

The authors report no conflicts of interest related to the present work. The research program of Dr. Baumann is generously supported by the Intramural Research Program of the National Institute on Drug Abuse, National Institutes of Health, grant DA 000523-13.

ADDITIONAL INFORMATION

Supplementary information The online version contains supplementary material available at https://doi.org/10.1038/s41386-021-01227-8.

Correspondence and requests for materials should be addressed to Michael H. Baumann.